Understanding the Scale Relationships of Uncertainty Propagation of Satellite Rainfall through a Distributed Hydrologic Model

EFTHYMIOS I. NIKOLOPOULOS AND EMMANOUIL N. ANAGNOSTOU

Civil and Environmental Engineering, University of Connecticut, Storrs, Connecticut, and Institute of Inland Waters, Hellenic Centre for Marine Research, Anavissos, Greece

FAISAL HOSSAIN

Civil and Environmental Engineering, Tennessee Technological University, Cookeville, Tennessee

MEKONNEN GEBREMICHAEL

Civil and Environmental Engineering, University of Connecticut, Storrs, Connecticut

MARCO BORGA

Department of Land and Agroforest Environment, University of Padova, Padova, Italy

(Manuscript received 10 March 2009, in final form 5 December 2009)

ABSTRACT

The study presents a data-based numerical experiment performed to understand the scale relationships of the error propagation of satellite rainfall for flood evaluation applications in complex terrain basins. A satellite rainfall error model is devised to generate rainfall ensembles based on two satellite products with different retrieval accuracies and space–time resolutions. The generated ensembles are propagated through a distributed physics-based hydrologic model to simulate the rainfall–runoff processes at different basin scales. The resulted hydrographs are compared against the hydrograph obtained by using high-resolution radar rainfall as the ''reference'' rainfall input. The error propagation of rainfall to stream runoff is evaluated for a number of basin scales ranging between 100 and 1200 km^2. The results from this study show that (i) use of satellite rainfall for flood simulation depends strongly on the scale of application (catchment area) and the satellite product resolution, (ii) different satellite products perform differently in terms of hydrologic error propagation, and (iii) the propagation of error depends on the basin size; for example, this study shows that small watersheds (<400 km^2) exhibit a higher ability in dampening the error from rainfall to runoff than larger-sized watersheds, although the actual error increases as drainage area decreases.

1. Introduction

Precipitation is one of the most important components of the hydrological cycle and the driving force for one of the most devastating natural hazards—that is, floods. Model simulation of the hydrologic processes (e.g., the generation of runoff) at watershed scale is the basis for nowcasting floods and providing information that is essential for the preservation of property and human lives. The primary input to a hydrological model is precipitation. Consequently, the accuracy of the flood prediction is tied to the accuracy of the precipitation estimation. However, estimating rainfall rates at high accuracy and continuously in space and time is an extremely difficult task because of the limitations of current sensor technologies, both in terms of resolution and spatiotemporal coverage, as well as uncertainty in the inversion techniques.

Traditionally, rain gauges have been used to measure surface rainfall rates. Gauges are considered as the most accurate sensors for measurements over a limited area (nearly a point), but their small coverage (especially over complex terrain and tropical regions) limits the adequacy

Corresponding author address: Emmanouil N. Anagnostou, Department of Civil and Environmental Engineering, University of Connecticut, Unit 2037, Storrs, CT 06269.
E-mail: manos@engr.uconn.edu

DOI: 10.1175/2009JHM1169.1

in representing the spatial structure of highly variable rainfall fields over large spatial scales. Weather radars, on the other hand, have advanced precipitation monitoring because of the spatially distributed information these systems can provide, and they have created significant potential on the use of radar observations for flood-related applications (Tilford 1987; Garrote 1992; Pessoa et al. 1993; Borga et al. 2000; among others). Radar rainfall estimates also suffer from a number of uncertainties associated with issues in radar calibration, variability in the reflectivity-to-rainfall relationship, vertical reflectivity profile, and atmospheric/rain-path attenuation [more details on the issue can be found in Krajewski and Smith (2002)]. Furthermore, beam blockage effects due to complex terrain constrain the applicability of radar observations in mountainous areas (mostly prone to flooding), while the establishment of a network of sensors that could resolve the coverage issue is rarely a viable solution because of the high cost of deploying such systems.

In recent times, there has been significant development in space-based precipitation estimation that has now opened up new horizons in hydrological applications at global scale. Satellite sensors offer unique advantages compared to gauges and weather radars because they provide (i) global coverage and (ii) observations in regions where in situ data are inexistent or sparse. Because of this uniqueness, the use of satellite data for hydrologic applications has gained growing interest. Guetter et al. (1996) conducted numerical experiments using synthetic satellite rainfall data, forcing a rainfall–runoff model to estimate soil water and streamflow at three large-scale basins (>2000 km^2) in the United States. Tsintikidis et al. (1999) examined the potential use of visible and infrared images to derive mean areal rainfall estimates to force a hydrologic model in the Blue Nile region. Wilk et al. (2006) used passive microwave datasets to derive estimates of the water balance over the Okavango basin. Su et al. (2008) evaluated the use of Tropical Rainfall Measuring Mission (TRMM) Multisatellite Precipitation Analysis product (3B42) for streamflow simulations in the La Plata basin. In a similar manner, Collischonn et al. (2008) used the 3B42 dataset to estimate daily streamflow in the Amazon basin.

Although these studies revealed the potential on the use of satellite-based rainfall estimates for hydrologic applications, they also reported deficiencies that differ in significance depending on the use. The two main sources of those deficiencies are (i) the error structure of the satellite rainfall estimates and (ii) the rainfall error propagation through the hydrologic model. For the first source, several studies have been reported that deal with the assessment and the characterization of the retrieval error for a number of global satellite rainfall products (see McCollum et al. 2002; Gebremichael and Krajewski 2004; Ebert et al. 2007; Dinku et al. 2007; among others). Although these studies provide useful information on satellite rainfall uncertainties, as Hossain and Anagnostou (2006a) pointed out, they focus on the accumulation of rainfall over large spatiotemporal scales as opposed to the flux, involving error statistics that are more relevant to large-scale meteorological phenomena. Hence, many of these studies do not provide insight on the smaller-scale surface hydrologic processes, such as floods and flash floods, particularly over complex terrain (see, e.g., Griffith et al. 1978; Arkin and Meisner 1987; Huffman et al. 2001; Steiner et al. 2003; among others). Hossain and Anagnostou (2006b) and Bellerby and Sun (2005) are some of the examples of recent effort to address this issue of characterizing the satellite error structure at scales relevant to flood processes.

On the second error source, the propagation of error in rainfall through a hydrologic model is a subject that has long been identified as a critical issue. However, most studies so far have involved the propagation of radar rainfall error (see, e.g., Borga et al. 2000; Borga 2002; Sharif et al. 2004; Vivoni et al. 2007), and only a few studies have investigated the satellite rainfall error propagation in hydrologic simulations (Hossain and Anagnostou 2004, 2005; Hong et al. 2006, 2007; Nijssen and Lettenmaier 2004). Evaluating the error propagation of satellite rainfall through the prism of surface hydrology is a very challenging task because it relates too many factors, which include among others (i) specifications of the satellite rainfall product, (ii) scale of the basin, (iii) spatiotemporal scale of the hydrologic variable of interest, (iv) the level of complexity and physical processes represented by the hydrologic model used, and (v) regional characteristics. As we now stand at the doorstep of a global-scale precipitation mission, named Global Precipitation Measurement (GPM, available online at http://gpm.gsfc.nasa.gov/; Smith et al. 2007), a comprehensive investigation/evaluation of the use of current satellite products in small-scale hydrologic applications appears mandatory and can serve as a valuable reference to the mission's designers as well as highlight its usefulness to society.

This paper aims to evaluate the scale characteristics of satellite rainfall error propagation through a distributed hydrologic model, with an emphasis on flood simulations over complex terrain. Because the surface hydrologic processes leading to surface runoff generation are controlled by the complexity of the terrain, the use of a distributed and physically based model is a necessary, but it is often an absent ingredient in literature on error propagation. The general framework of this study follows the

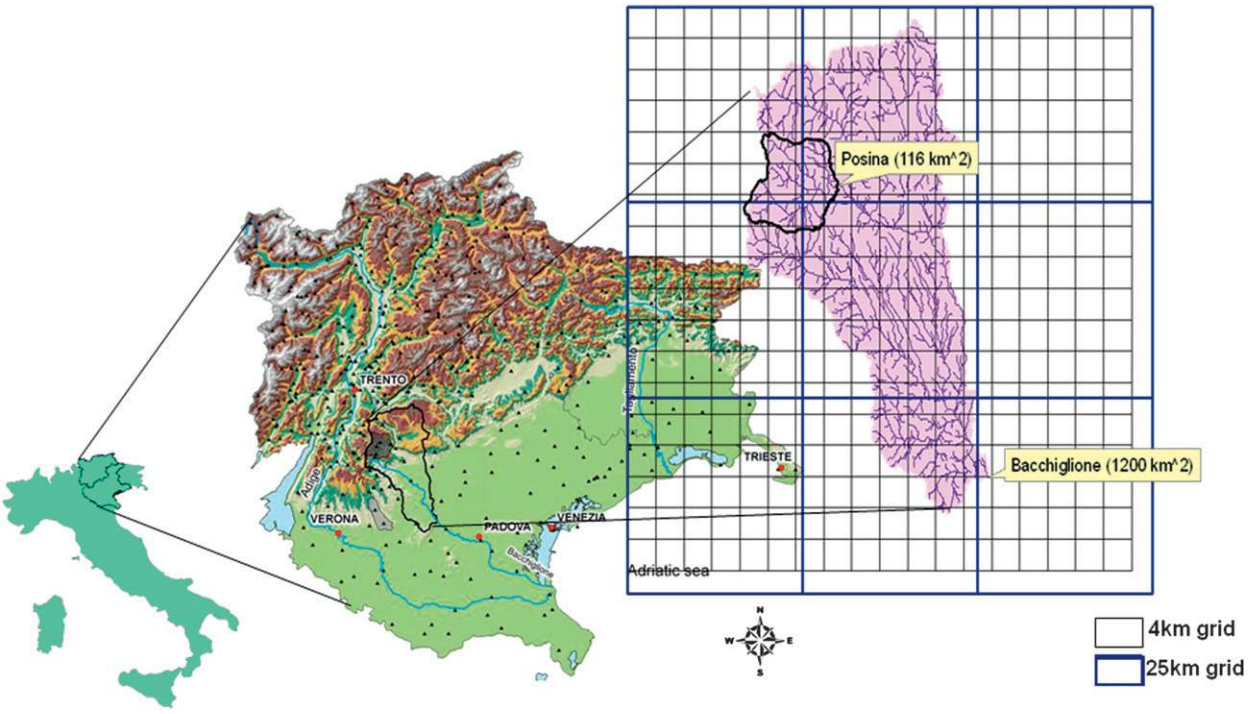

FIG. 1. Map showing the locations of the Posina and Bacchiglione basins in the northeastern Italian Alps. Note that the thin (4 km) and thick (25 km) grids provide a visual comparison between the spatial resolution of the satellite products used and the basin scales.

work by Hossain and Anagnostou (2004) and Hong et al. (2006), in the sense that an error model is used for the generation of ensembles of satellite rainfall fields, which subsequently propagate through a hydrologic model to evaluate the runoff error in a probabilistic manner. The most notable novelty of our work is the higher level of complexity in terms of both the satellite rainfall error model and hydrologic model used as well as the fact that two satellite products with contrasting space–time scales are examined. Furthermore, the scale dependence of the error propagation is addressed and investigated by comparing the results for a number of basins ranging from 100 to 1200 km^2. Results in this study are based on a single flood event that took place in a mountainous basin in northeast Italy. Although it is recognized that results can be driven by the specific characteristic of the analyzed event, we hope that this paper will provide a proof of concept to trigger further studies that will involve a wide range of systematic investigations with hydrologic models of varying complexity, storm cases of different spatiotemporal rainfall variability, basins of varying characteristics, and satellite products of varying resolutions and error characteristics.

In section 2 the study area and the datasets utilized in this study are presented. The methodology for the generation of satellite rainfall ensembles along with an error analysis is described in section 3, and the resulted simulated hydrographs from the propagation of those ensembles is discussed and analyzed in section 4. The main results of the error propagation analysis are described in section 5, and overall conclusions are summarized in section 6.

2. Study area and data

The basin—Bacchiglione basin—considered in this study is located in the Veneto region, which is part of the northeastern Italian Alps (Fig. 1). An area of approximately 1200 km^2 drains to its outlet just upstream from the city of Montegaldella, with a drainage direction that has a north–south alignment. The variability of the terrain is very distinct, with the upper part (first 30 km from the northern boundary of the basin) being highly irregular with an elevation that ranges from 200 to greater than 2000 m, and the mid-to-lower part being quite flat (elevation around 100 m and slopes lower than 0.5°). The vegetation follows in a sense the elevation pattern and differentiates between forested (broadleaf and conifer) areas in the higher elevation region (northern basin, which is part of the eastern Italian Alps) and the lower elevation (mid-to-lower basin) that is predominately covered by croplands. The high precipitation amounts in the area (>1000 mm annually) along with the very steep irregular terrain (slopes greater than 40° in the highlands)

make the region prone to the generation of floods and thus suitable for hydrologic investigations.

Several sources of data are utilized in this study. The precipitation data included both in situ measurements (rain gauges) and remote sensing–based (radar and satellite) retrievals. The rain gauges, located in the region (see Fig. 1), provided half-hourly rainfall accumulations that were used for (i) bias adjustment of the radar rainfall fields (Borga et al. 2000) and (ii) calibration of the satellite rainfall error model (Hossain et al. 2009). Distributed rainfall maps are obtained from a C-band Doppler weather radar located at Mt. Grande, approximately 10 km southeast of the basin's outlet, and were available at 1-km spatial and 1-h temporal resolution. The algorithm used to generate rainfall estimates from those radar measurements and performance evaluations are described in Borga et al. (2000). Two different satellite products were used: the TRMM 3B42 version 6 (Huffman et al. 2007) and a dataset obtained from the calibration of high-resolution global IR data from available passive microwave satellite rainfall estimates on the basis of the algorithm described in Kidd et al. (2003), hereafter named KIDD. Table 1 summarizes the native space–time resolution of each precipitation dataset used in this study. The hydrologic data include stream gauge observations that were available at half-hourly scale but only for one subbasin (called Posina; see Fig. 1). Furthermore, soil and land use/cover maps were used to derive the soil and vegetation properties required for the successful hydrologic model setup.

TABLE 1. Nominal spatial and temporal resolution of the precipitation data used.

Data type	Product name	Resolution	
		Temporal (h)	Spatial
Remote sensing	3B42	3	0.25° × 0.25°
	KIDD	0.5	~4 × 4 km
	Radar	1	1 km
In situ	Gauge	0.5	Point

3. Satellite rainfall ensembles

We used the satellite rainfall error model developed by Hossain and Anagnostou [2006b; a two-dimensional satellite rainfall error model (SREM2D)]. SREM2D uses stochastic space–time formulations to characterize the multidimensional error structure of satellite retrievals and combines that with input ''reference'' rain fields (representing the ''true'' surface rainfall process) of higher accuracy and resolution to simulate probable realizations of satellite like rainfall estimates [for more details on the error model, see Hossain and Anagnostou (2006b)]. One of the model prerequisites is the regional calibration for every satellite product; this means that for the simulation of each satellite product, a different set of parameters needs to be obtained. In our case, the model parameters were calibrated for the study region using six months (June–November 2002) of gauge and satellite data for the 3B42 and KIDD satellite rainfall products. The calibration of SREM2D parameters and the verification of the predicted variability for the region and satellite products used in this study are described in Hossain et al. (2009). The focus of this paper is on the analysis of the generated ensembles from the SREM2D error model and their error propagation.

The high-resolution (1 km–1 h) radar rainfall fields were used as the reference to generate realizations for (i) the 3B42 product at its nominal scale (see Table 1), (ii) the KIDD product at high resolution (4 km–1 h, hereafter KIDD-4 km), and (iii) the KIDD product aggregated at coarser space–time resolution (25 km–3 h, hereafter KIDD-25 km). The reason for aggregating the KIDD product was to compare the error propagation characteristics of (i) the two satellite products at the same resolution (3B42 versus KIDD-25 km) and (ii) the two resolutions for the same product (KIDD-4 km versus KIDD-25 km). A total of 100 realizations were generated for each satellite product; however, because of computational limitations, subsamples of those realizations were used to force the hydrologic model. This was done in the following procedure. Ensembles of each satellite product were ranked based on their overall rainfall bias (compared to the reference field), and realizations were selected starting at the fifth percentile with a step increment of five percentiles (5th, 10th, 15th, etc.). Thus, a total of 20 realizations (see Figs. 2 and 3) plus the average of all 100 realizations from each set were used for the error propagation experiment.

The results presented in this study are focused on a major flood event that occurred in the study area during October 1996 [started around 15:00 central European time (CET) 15 October]. The rainfall event that caused the flooding lasted for more than 60 hours and resulted in mean areal rainfall accumulation (based on radar estimates) of 200 mm for the Bacchiglione basin (~1200 km^2) and approximately 350 mm (see Figs. 2 and 3) for the mountainous subbasin of Posina (~116 km^2). In Figs. 2 and 3, we present the mean areal precipitation (MAP) derived from reference (radar) and from the SREM2D ensembles for the Bacchiglione and Posina basins, respectively. MAP was calculated during a 96-h window that extended a few hours before and after the flood-induced storm. Mean areal precipitation for each basin was based on the arithmetic average of all pixels (radar

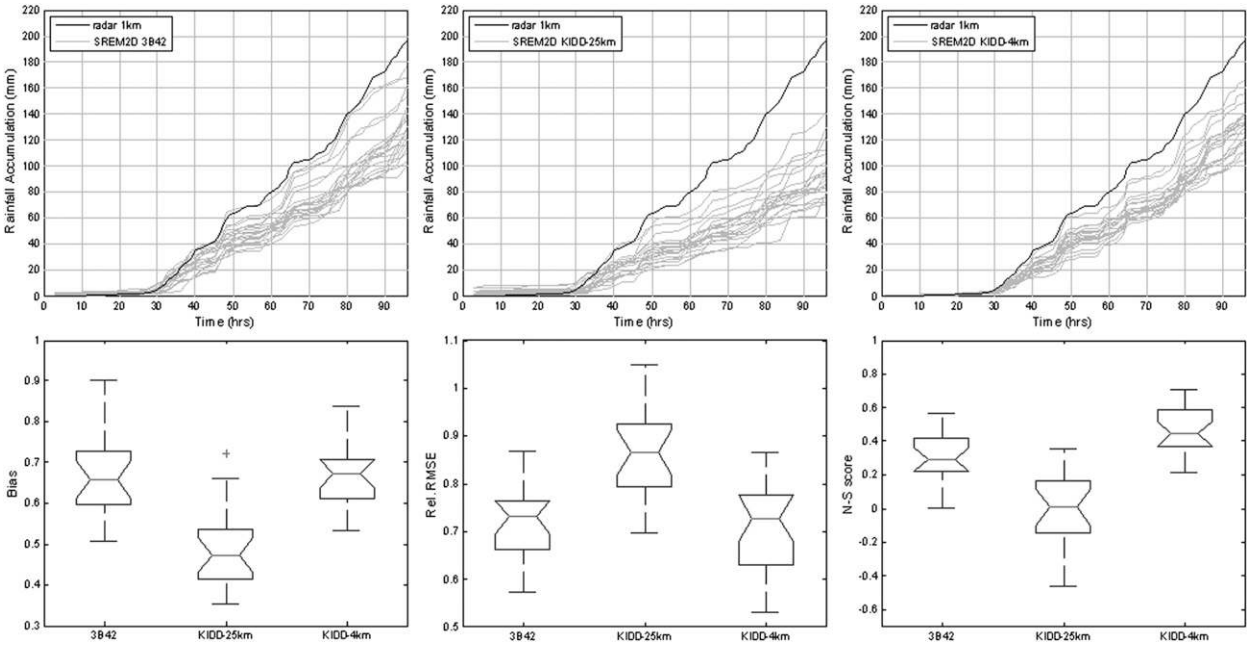

FIG. 2. (top) Mean areal rainfall accumulation curves for Bacchiglione basin calculated from radar (black) and SREM2D ensembles for (left) 3B42, (middle) KIDD-25 km, and (right) KIDD-4 km. (bottom left) Bias, (middle) relRMSE, and (right) N–S score between MAP time series derived from SREM2D ensembles and the reference rainfall (radar).

or satellite) that fully or partially overlapped the basin's area. Because of the high resolution of radar fields (1 km) and the relatively large area of the basin examined (>100 km; see Table 2), areal weighting was not applied for the calculation of the reference MAP but only for the satellite rainfall MAP (for all products). The generated ensembles are compared with the reference rainfall, and the results are presented as box plots of bias, relative root-mean-square error (relRMSE), and Nash–Sutcliffe (N–S) score defined as

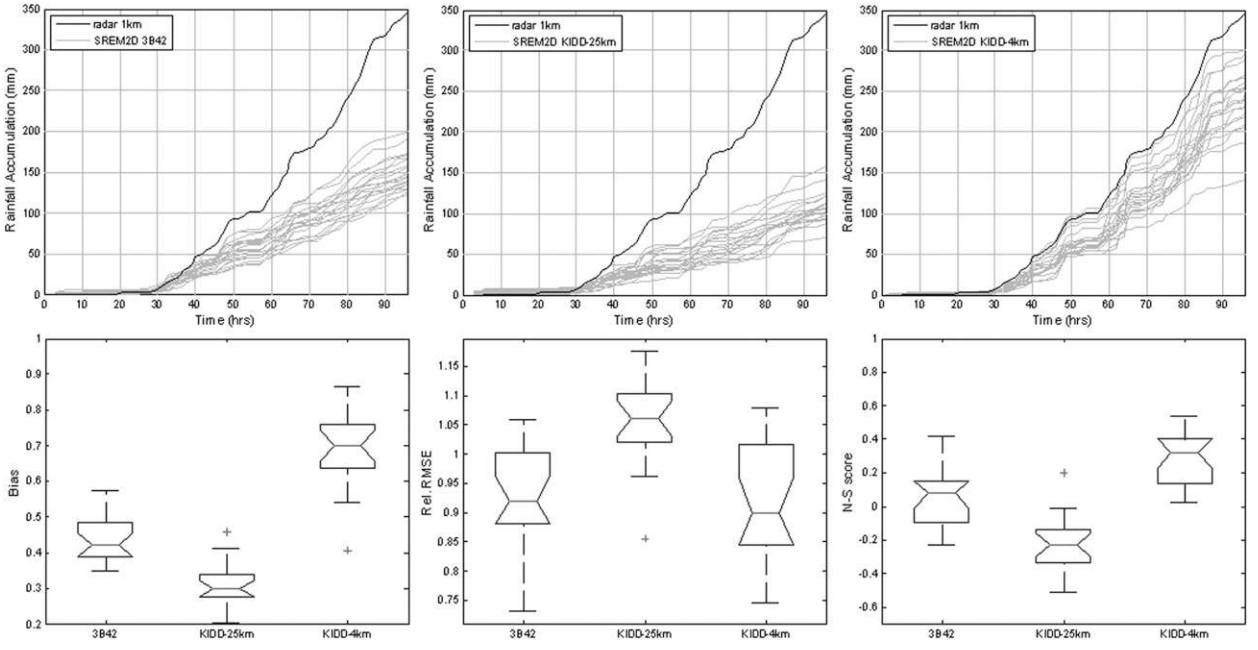

FIG. 3. Same as Fig. 2 but for the Posina basin.

TABLE 2. List of size and topography slope information of the basins used in this study.

Basin	Area (km^2)	Slope (°)	
		Mean	Std dev
1	108	5.07	4.8
2	148	12.45	8.85
3	244	11.02	7.37
4	269	9.59	9.03
5	398	13.55	9.27
6	584	15.24	9.89
7	627	14.87	9.83
Posina	116	20.61	9.23
Bacchiglione	1200	10.57	9.82

$$\text{Bias} = \frac{\sum_{i=1}^{N} X_{\text{SREM2D}}(i)}{\sum_{i=1}^{N} X_{\text{RADAR}}(i)}, \tag{1}$$

$$\text{RelRMSE} = \frac{\sqrt{\dfrac{\sum_{i=1}^{N} [X_{\text{RADAR}}(i) - X_{\text{SREM2D}}(i)]^2}{N}}}{\dfrac{\sum_{i=1}^{N} X_{\text{RADAR}}(i)}{N}}, \quad \text{and} \tag{2}$$

$$\text{N–S} = 1 - \frac{\sum_{i=1}^{N} [X_{\text{RADAR}}(i) - X_{\text{SREM2D}}(i)]^2}{\sum_{i=1}^{N} [X_{\text{RADAR}}(i) - \overline{X}_{\text{RADAR}}(i)]^2}, \tag{3}$$

where $X_{\text{RADAR}}(i)$ and $X_{\text{SREM2D}}(i)$ correspond to the time series of MAP (or streamflow for later use) at an hourly time step i obtained from radar and SREM2D ensembles, respectively. Here N is the total number of hourly time steps in $\mathbf{X}_{\text{RADAR}}$ and $\mathbf{X}_{\text{SREM2D}}$, and $\overline{\mathbf{X}}_{\text{RADAR}}$ denotes the arithmetic average of $\mathbf{X}_{\text{RADAR}}$.

Several points are noted from Figs. 2 and 3. First, all satellite realizations underestimate the total reference rainfall (bias <1). However, the magnitude of the underestimation depends strongly on the satellite product and on the scale of the basin. Specifically, for the larger basin (Bacchiglione), the 3B42 and KIDD-4 km perform equally well with a bias about 0.6–0.7, whereas the KIDD-25 km has a bias in the range of 0.4–0.5. For the smaller basin (Posina), the KIDD-4 km outperforms 3B42, while the aggregated KIDD-25 km is the worse of the three. The relative RMSE and the N-S score show similar behavior. This scale dependence of the error can be explained by the fact that coarse-resolution products (e.g., 3B42) cannot represent well the mean areal precipitation of basins with areas much smaller than their pixel size (see Fig. 1), simply because their sampling involves a much larger area.

The comparison between 3B42 and KIDD-25 km denotes the difference in retrieval error of two satellite algorithms, whereas the comparison between KIDD-4 km and KIDD-25 km denotes the resolution effect. We note that a product with higher retrieval error, but higher resolution (KIDD-4 km), can match (for the case of Bacchiglione) a product with lower retrieval error but with coarser resolution (3B42)—and even outperforming it at the small-scale basin (case of Posina). This outcome can serve as a reference to the satellite retrieval community, because it points out the necessity of having high-resolution products for the efficient use of satellite rainfall in hydrologic applications, especially for small-scale phenomena, such as flash floods, even by compromising the accuracy of the retrieval. Moreover, efforts regarding the improvement of satellite rainfall retrievals must continue because as we can observe from the results, satellite rainfall for all products is associated with high bias (>30%) and reduced ability to characterize the ''true'' process (N − S < 0.5).

4. Hydrologic simulations

The hydrologic model used in this study [triangulated irregular network (TIN)-based Real-time Integrated Basin Simulator (tRIBS)] is a fully distributed model that can simulate multiple storm events and account for the moisture losses during interstorm periods [see Ivanov et al. (2004) for more details]. tRIBS has been applied successfully to several flood-related studies (e.g., Vivoni et al. 2006a,b) that demonstrate the ability of the model to represent the hydrologic response during extreme events. A recent application of tRIBS to describe the hydrological processes of flash floods in mountainous basins was reported by E. I. Nikolopoulos et al. (2010, unpublished manuscript) for one of the subbasins (Posina) of the herein study area. One of the major advantages of using tRIBS is its ability to represent the complex terrain with high accuracy while being computationally very efficient (reduced number of computational nodes) by leveraging the triangulated irregular network's scheme (Vivoni et al. 2004, 2005). This attribute is very important when ensemble simulations are considered (e.g., Forman et al. 2008; Mascaro et al. 2010). In our case study, we used the model to simulate a single storm-induced flood event (the October 1996 flood). The distributed nature of the model allows retrieving the hydrograph response for several interior nodes of the basin,

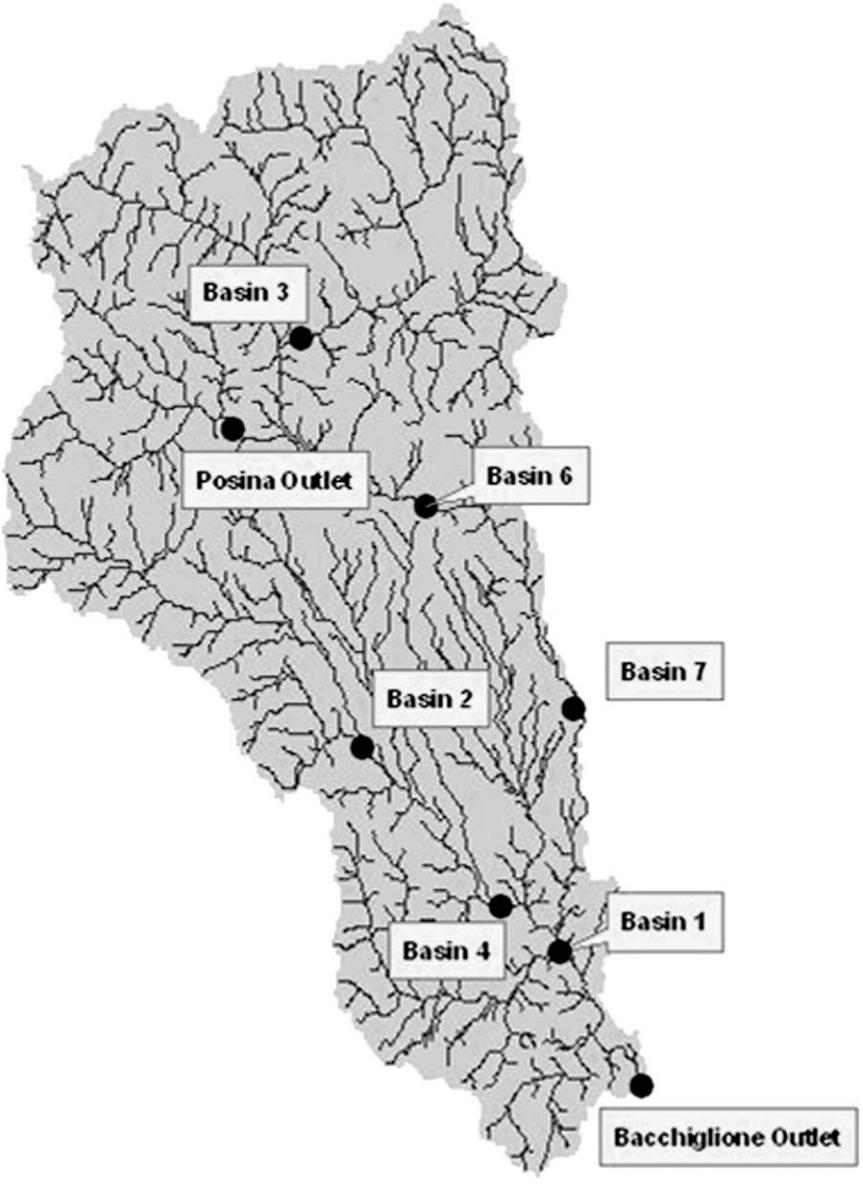

FIG. 4. Stream network of the Bacchiglione basin and the locations (black dots) of the basin outlets analyzed in this study. Note that the numeric identifications (IDs) correspond to the IDs presented in Table 2.

thus providing the ability to compare the error propagation for different scales of drainage area. In this study, we evaluated the error propagation for a number of basin scales that ranged between 100 and 1200 km^2 (see Fig. 4; Table 2).

The successful setup of this type of model requires detailed information regarding the land descriptors (land use/cover, soil type, etc.) of the simulation domain. The Bacchiglione basin was categorized into four major land use/cover classes that include barren land, grass, broadleaf forests, and conifer forests and into three soil classes based on the general pattern of land use/cover. For the parameterization of the soil and land cover variables in the model, we relied on different sources found in the literature (Jury et al. 1991; available online at http://ldas.gsfc.nasa.gov/). To ensure that the model could properly describe the rainfall–runoff transformation processes of the flood event used in this simulation exercise, we carried out a minimal calibration of only 3 (out of approximately 30) parameters for which the flood hydrograph was most sensitive and relied on values derived from the literature for the remaining parameters. The

TABLE 3. Calibrated parameters of saturated hydraulic conductivity, conductivity decay coefficient, and anisotropy ratio for the three soil classes of the Bacchiglione basin.

Soil class	Saturated hydraulic conduct (mm h^{-1})	Conductivity decay coefficient ($\times 10^{-4}$)	Anisotropy ratio
A	28	7.75	620
B	22.5	6.56	144
C	29	4.96	183

parameters that were calibrated were the saturated hydraulic conductivity, the conductivity exponential decay coefficient, and the anisotropy ratio (defined as the ratio of horizontal to vertical hydraulic conductivity). The model was forced with the reference (radar) rainfall input, and the shuffle complex evolution (SCE) optimization method (Duan et al. 1992) was used to minimize the mean squared error between the observed and the simulated hydrograph. The calibration was performed on the flood event used in this study, and as mentioned earlier, the only available hydrograph measurements for the basin were at the Posina outlet. Thus, instead of using the model's output at the outlet of the domain (Bacchiglione basin), we used the interior simulations that corresponded to the Posina subbasin and compared those to the available observations. Note that the total simulation time was 160 h, and all the runoff quantities presented herein were calculated over that time window. Table 3 shows the final calibrated values of the three parameters, and Fig. 5 presents a comparison of the simulated (based on calibrated parameters) and observed hydrographs. While the simulated hydrograph appears to be more sensitive to rainfall variations than the observed, the general response is realistic and associated with a relative error of ~20% for the peak discharge, which is low relative to the range of runoff simulation errors associated with the herein error propagation experiment. A point to note is that the main objective of the calibration exercise presented here was to ensure that the transformation of rainfall to runoff for the specific event would be as realistic as possible because that would have an effect on the results of the error propagation analysis. Thus, we do not claim that the calibration exercise presented here provides a model suitable for general flood prediction of storm cases in this basin.

The calibrated hydrologic model was forced with the generated SREM2D ensembles from each satellite rainfall product, and the simulated hydrographs for all nine basins (Table 2) were analyzed. Figures 6 and 7 show the corresponding hydrographs for the rainfall ensembles presented in Figs. 2 and 3, respectively. As expected, the conclusions derived from the comparison between the SREM2D-derived hydrographs and the reference is

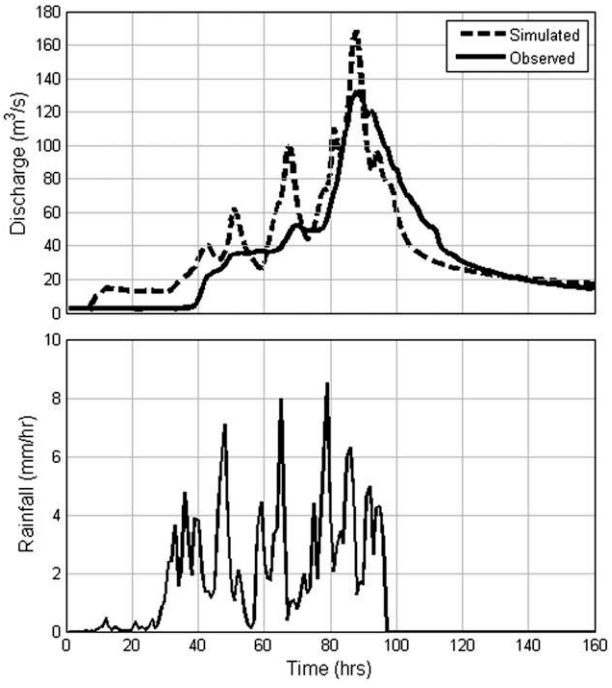

FIG. 5. (top) Observed (solid) and simulated (dashed) hydrographs for the Posina basin during the October 1996 flood event. (bottom) MAP over the Posina basin based on radar rainfall data.

in agreement with the comparison of the rainfall fields. Again, 3B42 and KIDD-4 km behave similarly and significantly better than the KIDD-25 km for the large-scale (Bacchiglione) basin, whereas for the smaller-scale basin (Posina), the hydrologic simulations based on the high-resolution KIDD-4 km product outperforms all other products. An interesting point to note is that for the larger basin (Bacchiglione), the 3B42 exhibits higher variability (larger whisker lengths of the boxplots) than the KIDD-4 km in bias and N-S score, whereas for the smaller basin (Posina) this is reversed. However, this difference is not that apparent in the variability of rainfall statistics (Fig. 3), which indicates that the rainfall-to-runoff transformation can magnify (or attenuate) the variability in rainfall retrieval error. The spread of the simulated hydrographs corresponds to the uncertainty in hydrologic simulations due to uncertainty in rainfall; therefore, based on the earlier-mentioned findings, the propagation of rainfall uncertainty depends significantly on basin scale and hydrologic response (i.e., dominant runoff generation mechanisms). This is discussed next.

5. Analysis of error propagation

To investigate the propagation of error in satellite rainfall through the rainfall–runoff transformation, the

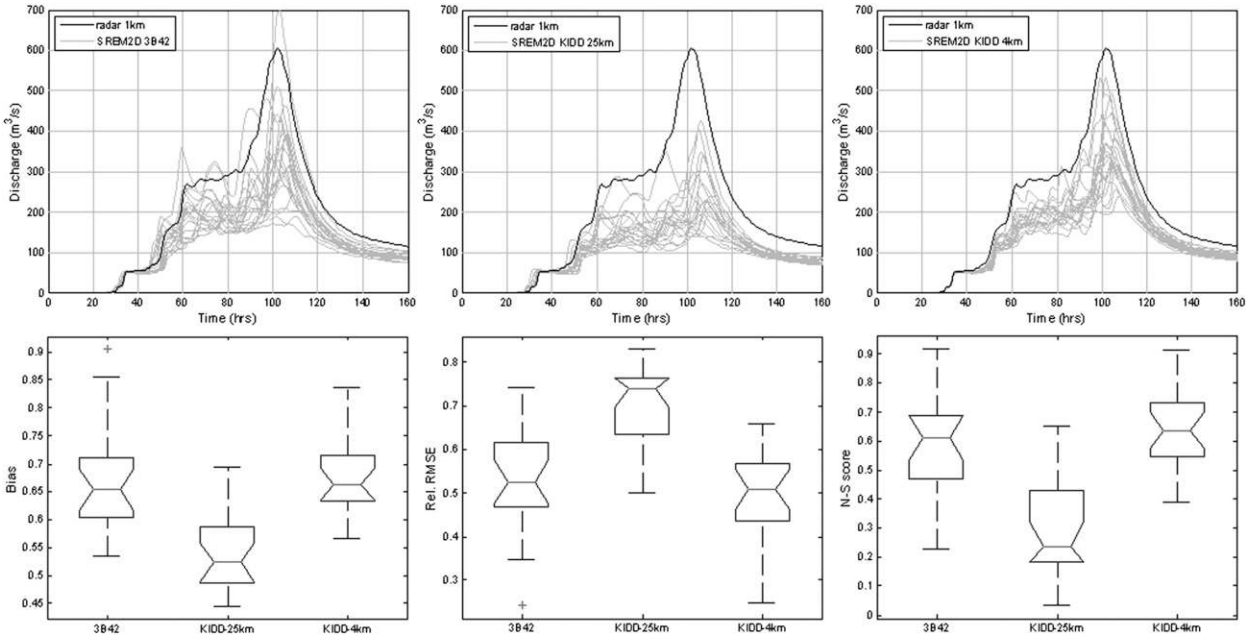

FIG. 6. (top) Simulated hydrographs based on radar (black) and SREM2D (gray) rainfall ensembles for (left) 3B42, (middle) KIDD-25 km, and (right) KIDD-4 km, for the Bacchiglione basin. (bottom left) Bias, (middle) rel. RMSE, and (right) N–S score between reference (radar) and SREM2D hydrographs.

error in rainfall versus error in runoff is presented in Fig. 8 based on the metrics of relative RMSE [Eq. (2)], and relative error defined as

$$\text{Relative Error} = \frac{\sum_{i=1}^{N} X_{\text{radar}}(i) - \sum_{i=1}^{N} X_{\text{SREM2D}}(i)}{\sum_{i=1}^{N} X_{\text{radar}}(i)}. \quad (4)$$

A very distinct feature of the results is that the propagation of error exhibits a linear behavior in terms of its relative term. This linearity appears stronger for the case of the Bacchiglione basin (1200 km^2). Especially for the scatterplot of relative errors in total rainfall versus relative errors in total runoff, the points are aligned very close to the 1:1 line, which indicates that the relative error in rainfall translates to an equal relative error in runoff. A point to note from Fig. 8 is that the performance of each satellite product manifests in distinct clusters of the rainfall–runoff error domain (those clusters are separated by different colors associated with different satellite products). This effect is much more profound in the case of Posina, where the points representing the high-resolution satellite product (KIDD-4 km, blue color) cluster in a distinct (from the other products) region in the figure that is associated with lower relative error and higher damping effect on the propagation of relative RMSE. For the Bacchiglione basin, the two clusters of KIDD-4 km and 3B42 mix in the same domain because they perform equally, as mentioned earlier. This strengthens the argument made in the previous section that for the smaller-scale basins, high-resolution products are critical to moderate the retrieval error propagation in runoff.

The propagation of rainfall error to peak runoff is also presented in Fig. 8. In the case of peak runoff, the propagation has a different effect compared to the total runoff. Most of the ensembles—for all products and both basins—show magnification of the relative error. For the Posina basin, the KIDD-4 km product shows high variability with the relative error in the peak discharge ranging between −20% and 50%, while the rainfall error is between 20% and 40%. This can be attributed to the highly nonlinear rainfall-to-runoff transformation and to the increased spatial variability of the high-resolution product, which, we speculate, can have a significant effect in the runoff production (especially for the highly complex terrain of Posina).

Similar analysis was carried out for all basins presented in Table 2, to further investigate the dependency of error propagation with basin scale. Results are presented in Fig. 9 in terms of the ratio of the error metric (relative error and relRMSE) in runoff over the corresponding error metric in rainfall versus basin scale. Ratios equal to one indicate that statistics of the error in rainfall would translate to an equal statistical measure of the error in runoff, whereas ratios lower (higher) than one would indicate that the error dampens (magnifies)

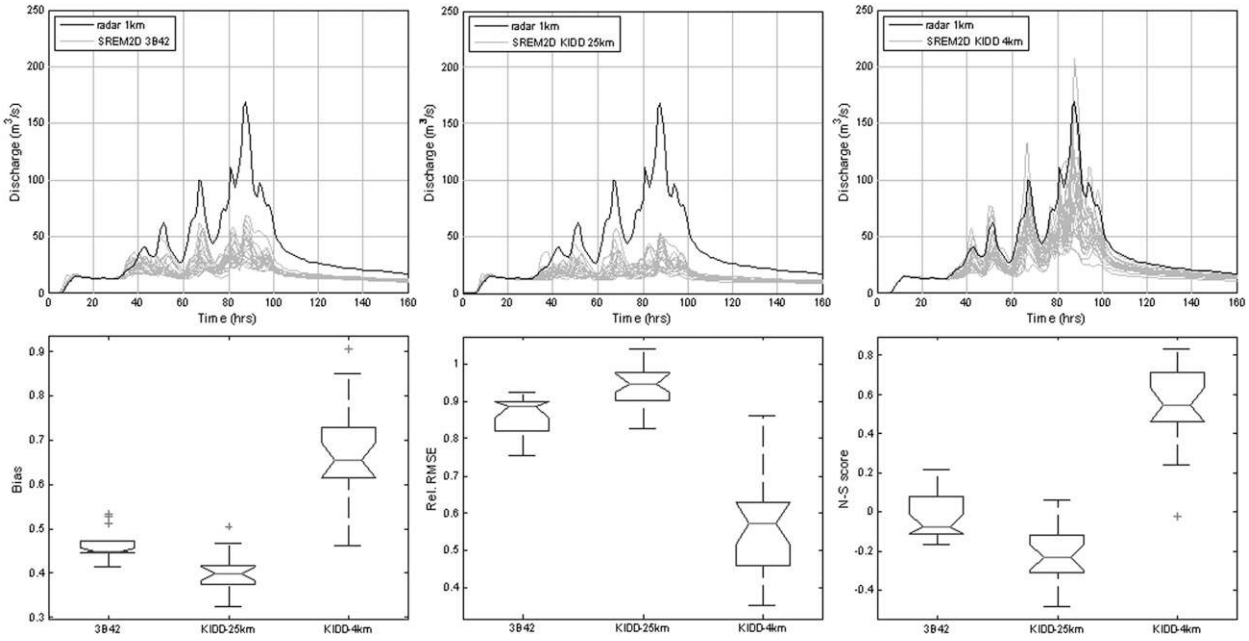

FIG. 7. Same as Fig. 6 but for the Posina basin.

through the rainfall–runoff transformation process. An increase of ratio with catchment area up to 600 km^2 and an approximate plateau for larger basins is consistent for all ratios presented in Fig. 9. These results clearly state the scale dependence of the propagation of error and indicate that for smaller-scale basins (<600 km^2), the damping effect of the error is greater than in larger basins. Moreover, the variability among products (scatter of solid circles) as well as the variability within each product (length of error bars) is higher for smaller-scale basins (<600 km^2) and consistent for all metrics. While all metrics exhibit similar trends, we need to point out that the magnification or damping of the error depends on the ''error metric'' itself. For example, the relative RMSE shows consistent damping (ratio <1) of the error from rainfall to runoff volumes at all scales, whereas the relative error magnifies from rainfall to peak runoff (ratio >1) in the majority of products and basin scales. Thus, one should clearly state the reference metric when deriving conclusions about the effect of rainfall error propagation on runoff simulations.

6. Conclusions

This paper presented results from a numerical experiment designed to evaluate the error propagation of satellite rainfall though a distributed hydrologic model to provide insight regarding the potential use of satellite rainfall for flood simulations. Our study focused on complex terrain wherein precipitation and the hydrologic process controls are strongly nonuniform and dictated by this complexity (in topography, vegetation, and soil properties). We used appropriate models to characterize this complexity in both the satellite rainfall error and the simulation of hydrologic processes. This stochastic data-modeling error framework allowed a probabilistic evaluation of the error propagation. The analysis was based on two satellite products at different resolutions and retrieval accuracies and a number of basins that ranged in scale (100–1200 km^2).

The principal conclusions of the study are summarized as follows:

1) The mean areal precipitation is consistently underestimated by satellite realizations. Bias can vary significantly depending on the product and the basin size. For the largest basin (Bacchiglione), 3B42 and KIDD-4 km performed equally well with bias around 0.6–0.7, whereas the KIDD-25 km dropped to 0.4–0.5. For the smaller-scale Posina basin, the KIDD-4 km maintains its performance, but the coarser-resolution products (3B42 and KIDD-25 km) give biases below 0.5. This is a clear indicator that the performance of a given product relates to both its resolution and scale of application.
2) The low N–S scores presented in the results indicate that satellite ensembles have low ability in characterizing the ''true'' process. This is essential, especially when we are interested in the hydrologic variability (e.g., runoff production) triggered by the rainfall forcing; because even if the bias in total rainfall can be low,

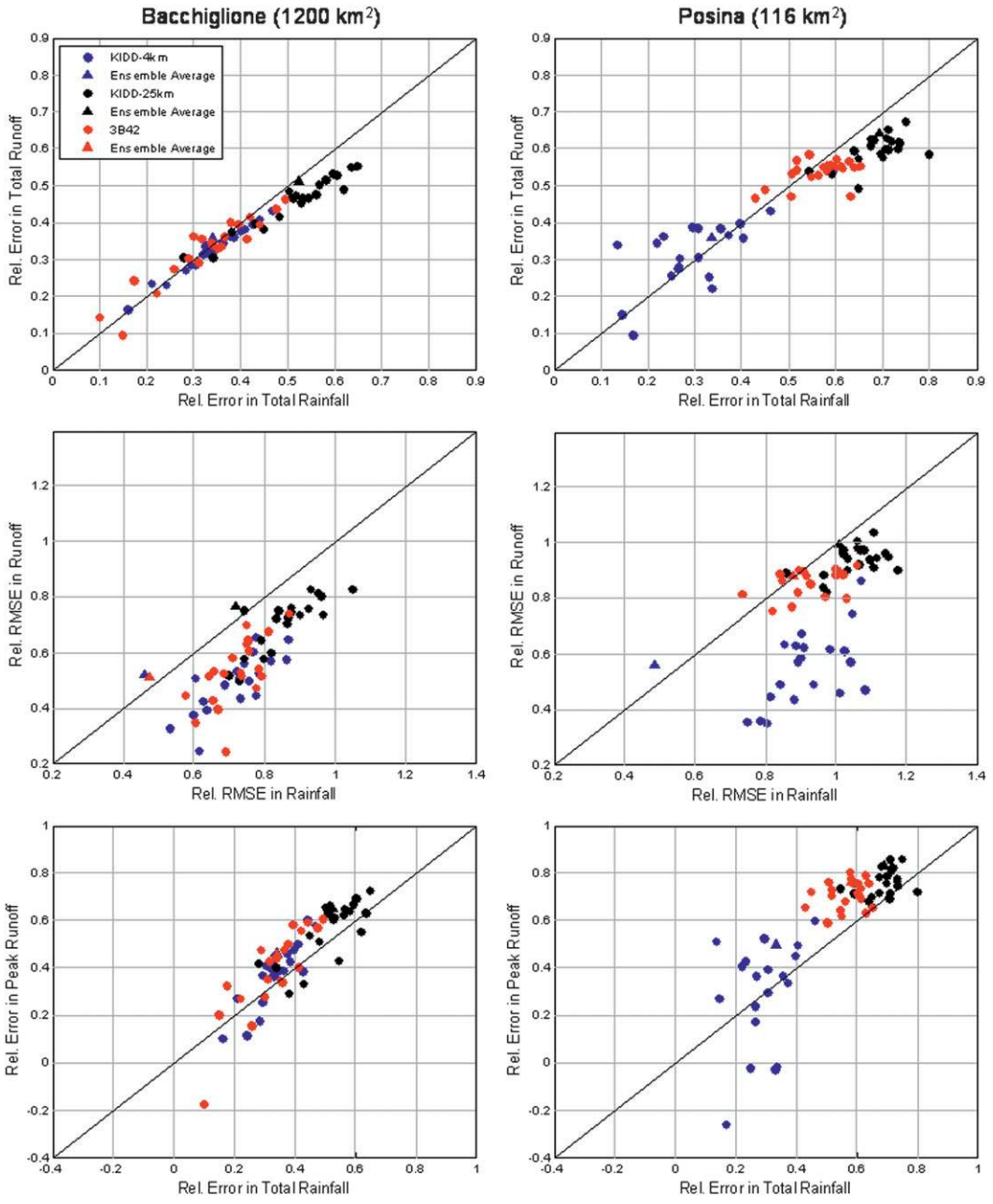

FIG. 8. Error propagation metrics: (top) relative error in total runoff vs relative error in total rainfall for the (left) Bacchiglione and (right) Posina basin, (middle) relRMSE in discharge vs relRMSE in rainfall, and (bottom) relative error in peak runoff vs relative error in total rainfall. Errors were calculated between SREM2D ensembles and the reference (radar). Note that the blue, black, and red triangles correspond to the ensemble average of KIDD 4 km, KIDD 25 km, and 3B42, respectively.

the distribution of that rainfall in space and time can alter significantly the hydrologic response at a basin.

3) The simulated hydrographs based on the satellite ensembles show the same behavior regarding the effect of resolution and basin scale. The highest resolution product (KIDD-4 km) outperforms the coarser-resolution products in all cases. This delivers a strong message to the satellite retrieval community about the necessity to provide high-resolution precipitation products for flood-related applications.
4) The propagation of error exhibits a linear behavior, especially for the larger-scale basins. The error's damping or magnification depends on the metric of reference. For example, the relative RMSE in

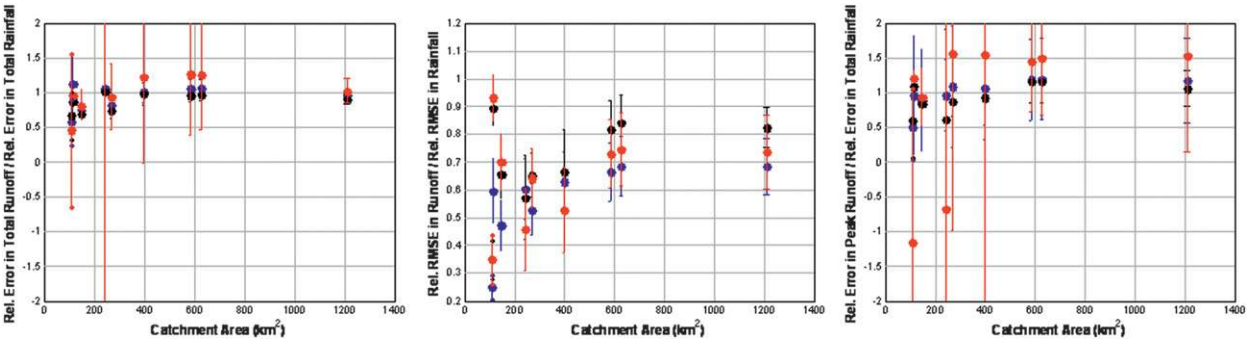

FIG. 9. Ratios of relative error in (left) total runoff and (right) peak runoff over relative error in total rainfall. (middle) Ratios of rel. RMSE in runoff over rel. RMSE in rainfall. All ratios are shown for different basin scales. The blue, black, and red circles correspond to the average of the 20 realizations for the KIDD 4 km, KIDD 25 km, and 3B42, respectively. Error bars are equal to ±1std dev.

rainfall propagates to a lower relative RMSE in runoff, whereas the relative error in total rainfall results in a magnified relative error in peak discharge (in most cases).

5) There is a definitive dependence of error propagation on basin scale. A consistent trend revealed in this study showed that the ability of dampening the error reduces as the basin scale increases and approaches a plateau for basins larger than 600 km^2.

As stated in the introduction, the findings of this study can be considered as a proof of concept regarding the use of satellite rainfall for complex terrain flood simulations. We acknowledge that the results presented herein are, to some extent, model dependent and strongly affected by the spatial structure of the specific storm rain patterns and basin characteristics (including antecedent conditions). However, our findings demonstrate a definitive potential in the use of satellite rainfall for flood simulations, and identify the key issues that require attention to further enhance that potential. For example, a point we make in this study is that product resolution is a critical issue for small-scale applications. Arguably, this makes the use of high-resolution IR-driven products, such as the Precipitation Estimation from Remotely Sensed Information using Artificial Neural Networks–Cloud Classification System (PERSIANN–CCS) neural network–based fusion technique (Hong et al. 2004) providing 4 km (½ h)$^{-1}$ rainfall fields, worthwhile for complex terrain flood simulations. On the other hand, the study also revealed a rather counterintuitive result, that error magnifies as a function of drainage area (and that there is a strong dependency on the metric used). To generalize and gain a holistic understanding of these issues, more systematic investigations of similar nature are needed to involve different satellite products, additional flood cases associated with varying storm and basin characteristics, and hydrologic models of varying complexity.

Acknowledgments. This work was supported by EU Marie Curie Excellence Grant Project PreWEC (MEXT-CT-2006-038331) and NASA Precipitation Measurement Mission award NNX07AE31G. E. I. Nikolopoulos was supported by a NASA Earth System Science Graduate Fellowship. Prof. Chris Kidd of the University of Birmingham provided the Kidd et al. (2003) satellite rainfall product. The TRMM 3B42 data were obtained from the Goddard Space Flight Center Distributed Active Archive Center's FTP site.

REFERENCES

Arkin, P. A., and B. N. Meisner, 1987: The relationship between large-scale convective rainfall and cold cloud cover over the Western Hemisphere during 1982–84. *Mon. Wea. Rev.,* **115,** 51–74.

Bellerby, T. J., and J. Sun, 2005: Probabilistic and ensemble representations of the uncertainty in an IR/microwave satellite precipitation product. *J. Hydrometeor.,* **6,** 1032–1044.

Borga, M., 2002: Accuracy of radar rainfall estimates for stream-flow simulation. *J. Hydrol.,* **267,** 26–39.

——, E. N. Anagnostou, and E. Frank, 2000: On the use of real-time radar rainfall estimates for flood prediction in mountainous basins. *J. Geophys. Res.,* **105** (D2), 2269–2280.

Collischonn, B., W. Collischonn, and C. E. M. Tucci, 2008: Daily hydrological modeling in the Amazon basin using TRMM rainfall estimates. *J. Hydrol.,* **360,** 207–216.

Dinku, T., P. Ceccato, E. Grover-Kopec, M. Lemma, S. J. Connor, and C. F. Ropelewski, 2007: Validation of satellite rainfall products over East Africa's complex topography. *Int. J. Remote Sens.,* **28,** 1503–1526.

Duan, Q., S. Sorooshian, and V. K. Gupta, 1992: Effective and Efficient Global Optimization for Conceptual Rainfall-Runoff Models. *Water Resour. Res.,* **28,** 1015–1031.

Ebert, E. E., J. E. Janowiak, and C. Kidd, 2007: Comparison of near-real-time precipitation estimates from satellite observations and numerical models. *Bull. Amer. Meteor. Soc.,* **88,** 47–64.

Forman, B. A., E. R. Vivoni, and S. A. Margulis, 2008: Evaluation of ensemble-based distributed hydrologic model response with disaggregated precipitation products. *Water Resour. Res.,* **44,** W12409, doi:10.1029/2008WR006827.

Garrote, L., 1992: Real-time modeling of river basin response using radar-generated rainfall maps and a distributed hydrologic

database. M.S. thesis, Dept. of Civil and Environmental Engineering, MIT, 501 pp.

Gebremichael, M., and W. F. Krajewski, 2004: Characterization of the temporal sampling error in space-time-averaged rainfall estimates from satellites. *J. Geophys. Res.,* **109,** D11110, doi:10.1029/2004JD004509.

Griffith, C. G., W. L. Woodley, P. G. Grube, D. W. Martin, J. Stout, and D. N. Sikdar, 1978: Rain estimation from geosynchronous satellite imagery—Visible and infrared studies. *Mon. Wea. Rev.,* **106,** 1153–1171.

Guetter, A. K., K. P. Georgakakos, and A. A. Tsonis, 1996: Hydrologic applications of satellite data: 2. Flow simulation and soil water estimates. *J. Geophys. Res.,* **101,** 26 527–26 538.

Hong, Y., K.-L. Hsu, S. Sorooshian, and X. Gao, 2004: Precipitation Estimation from Remotely Sensed Imagery using an Artificial Neural Network Cloud Classification System. *J. Appl. Meteor.,* **43,** 1834–1852.

——, ——, H. Moradkhani, and S. Sorooshian, 2006: Uncertainty quantification of satellite precipitation estimation and Monte Carlo assessment of the error propagation into hydrologic response. *Water Resour. Res.,* **42,** W08421, doi:10.1029/2005WR004398.

——, R. F. Adler, F. Hossain, S. Curtis, and G. J. Huffman, 2007: A first approach to global runoff simulation using satellite rainfall estimation. *Water Resour. Res.,* **43,** W08502, doi:10.1029/2006WR005739.

Hossain, F., and E. N. Anagnostou, 2004: Assessment of current passive-microwave- and infrared-based satellite rainfall remote sensing for flood prediction. *J. Geophys. Res.,* **109,** D07102, doi:10.1029/2003JD003986.

——, and ——, 2005: Numerical investigation of the impact of uncertainties in satellite rainfall estimation and land surface model parameters on simulation of soil moisture. *Adv. Water Resour.,* **28,** 1336–1350.

——, and ——, 2006a: Assessment of a Multidimensional Satellite Rainfall Error Model for Ensemble Generation of Satellite Rainfall Data. *IEEE Trans. Geosci. Remote Sens. Lett.,* **3,** 419–423.

——, and ——, 2006b: A two-dimensional satellite rainfall error model. *IEEE Trans. Geosci. Remote Sens.,* **44,** 1511–1522.

——, L. Tang, E. N. Anagnostou, and E. I. Nikolopoulos, 2009: A practical guide to a space-time stochastic error model for simulation of high-resolution satellite rainfall data. *Satellite Rainfall Applications for Surface Hydrology,* M. Gebremichael and F. Hossain, Eds., Springer, 145–167.

Huffman, G. J., R. F. Adler, M. M. Morrissey, D. T. Bolvin, S. Curtis, R. Joyce, B. McGavock, and J. Susskind, 2001: Global precipitation at one-degree daily resolution from multisatellite observations. *J. Hydrometeor.,* **2,** 36–50.

——, and Coauthors, 2007: The TRMM Multisatellite Precipitation Analysis (TMPA): Quasi-global, multiyear, combined-sensor precipitation estimates at fine scales. *J. Hydrometeor.,* **8,** 38–55.

Ivanov, V. Y., E. R. Vivoni, R. L. Bras, and D. Entekhabi, 2004: Catchment hydrologic response with a fully distributed triangulated irregular network model. *Water Resour. Res.,* **40,** W11102, doi:10.1029/2004WR003218.

Jury, W. A., W. R. Gardner, and W. H. Gardner, 1991: *Soil Physics*. 5th ed. John Wiley & Sons, 328 pp.

Kidd, C., D. R. Kniveton, M. C. Todd, and T. J. Bellerby, 2003: Satellite rainfall estimation using combined passive microwave and infrared algorithms. *J. Hydrometeor.,* **4,** 1088–1104.

Krajewski, W. F., and J. A. Smith, 2002: Radar hydrology: Rainfall estimation. *Adv. Water Resour.,* **25,** 1387–1394.

Mascaro, G., E. R. Vivoni, and R. Deidda, 2010: Implications of ensemble quantitative precipitation forecast errors on distributed streamflow forecasting. *J. Hydrometeor.,* **1,** 69–86.

McCollum, J. R., W. F. Krajewski, R. R. Ferraro, and M. B. Ba, 2002: Evaluation of biases of satellite rainfall estimation algorithms over the continental United States. *J. Appl. Meteor.,* **41,** 1065–1080.

Nijssen, B., and D. P. Lettenmaier, 2004: Effect of precipitation sampling error on simulated hydrological fluxes and states: Anticipating the Global Precipitation Measurement satellites. *J. Geophys. Res.,* **109,** D02103, doi:10.1029/2003JD003497.

Pessoa, M. L., R. L. Bras, and E. R. Williams, 1993: Use of weather radar for flood forecasting in the Sieve River basin: A sensitivity analysis. *J. Appl. Meteor.,* **32,** 462–475.

Sharif, H. O., F. L. Ogden, W. F. Krajewski, and M. Xue, 2004: Statistical analysis of radar rainfall error propagation. *J. Hydrometeor.,* **5,** 199–212.

Smith, E. A., and Coauthors, 2007: International Global Precipitation Measurement (GPM) program and mission: An overview. *Measuring Precipitation from Space: EURAINSAT and the Future,* V. Levizzani, P. Bauer, and F. J. Turk, Eds., Advances in Global Change Research Series, Vol. 28, Springer, 611–653.

Steiner, M., T. L. Bell, Y. Zhang, and E. F. Wood, 2003: Comparison of two methods for estimating the sampling-related uncertainty of satellite rainfall averages based on a large radar dataset. *J. Climate,* **16,** 3759–3778.

Su, F., Y. Hong, and D. P. Lettenmaier, 2008: Evaluation of TRMM Multisatellite Precipitation Analysis (TMPA) and its utility in hydrologic prediction in the La Plata Basin. *J. Hydrometeor.,* **9,** 622–640.

Tilford, K. A., 1987: Real-time flood forecasting using low intensity resolution radar rainfall data. M.S. thesis, Dept. of Civil Engineering, University of Birmingham, 67 pp.

Tsintikidis, D., K. P. Georgakakos, G. A. Artan, and A. A. Tsonis, 1999: A feasibility study on mean areal rainfall estimation and hydrologic response in the Blue Nile region using METEOSAT images. *J. Hydrol.,* **221,** 97–116.

Vivoni, E. R., V. Y. Ivanov, R. L. Bras, and D. Entekhabi, 2004: Generation of triangulated irregular networks based on hydrological similarity. *J. Hydrol. Eng.,* **9,** 288–303.

——, ——, ——, and ——, 2005: On the effects of triangulated terrain resolution on distributed hydrologic model response. *Hydrol. Processes,* **19,** 2101–2122.

——, R. S. Bowman, R. L. Wyckoff, R. T. Jakubowski, and K. E. Richards, 2006a: Analysis of a monsoon flood event in an ephemeral tributary and its downstream hydrologic effects. *Water Resour. Res.,* **42,** W03404, doi:10.1029/2005WR004036.

——, D. Entekhabi, R. L. Bras, V. Y. Ivanov, M. P. Van Horne, C. Grassotti, and R. N. Hoffman, 2006b: Extending the predictability of hydrometeorological flood events using radar rainfall nowcasting. *J. Hydrometeor.,* **7,** 660–677.

——, ——, and R. N. Hoffman, 2007: Error propagation of radar rainfall nowcasting fields through a fully distributed flood forecasting model. *J. Appl. Meteor. Climatol.,* **46,** 932–940.

Wilk, J., D. Kniveton, L. Andersson, R. Layberry, M. C. Todd, D. Hughes, S. Ringrose, and C. Vanderpost, 2006: Estimating rainfall and water balance over the Okavango River Basin for hydrological applications. *J. Hydrol.,* **331,** 18–29.